Electron Transfer between Two Silyl-Substituted Phenylene Rings: EPR/ENDOR Spectra, DFT Calculations, and Crystal Structure of the One-Electron Reduction Compound of a Di(*m*-silylphenylenedisiloxane)

Cosmina Dutan,† Sylvie Choua,† Théo Berclaz,† Michel Geoffroy,*,†
Nicolas Mézailles,‡ Audrey Moores,‡ Louis Ricard,‡ and Pascal Le Floch*,‡

*Contribution from the Department of Physical Chemistry, University of Geneva,
30 Quai Ernest Ansermet, 1211 Geneva 4, Switzerland, and
Laboratoire Hétéroéléments et Coordination, UMR CNRS 7653, Département de Chimie,
Ecole Polytechnique, 91128 Palaiseau Cedex, France*

Received July 1, 2002; Revised Manuscript Received January 17, 2003; E-mail: Michel.geoffrey@chiphy.unige.ch

Abstract: Reduction of a solution of octamethylcyclo-di(*m*-silylphenylenedisiloxane) **4** in THF on a potassium mirror leads to EPR/ENDOR spectra characterized by a large coupling (~20 MHz) with two protons, similar to the spectra obtained after reduction of the *m*-disilylbenzene derivative **5**, consistent with a localization of the extra electron on a single ring of **4**. The spectra recorded after reduction of **4** at low temperature in the presence of an equimolar amount of 18-crown-6 exhibit couplings of ~10 MHz with four protons and indicate that embedding the counterion in crown-ether provokes the delocalization of the unpaired electron on the two phenyl rings of **4**. The measured hyperfine interactions agree with those calculated by DFT for the optimized structure of **4**•⁻. Direct information on the structure of this anion is obtained from the X-ray diffraction of crystals grown at −18 °C in reduced solutions containing **4**, potassium, and crown ether in a THF/hexane mixture. Both DFT and crystal structures clearly indicate the geometry changes caused by the addition of an electron to **4**: the interphenyl distance drastically decreases, leading to a partial overlap of the two rings. The structure of **4**•⁻ is a model for an electron transfer (ET) transition state between the two aromatic rings. The principal reason for the adoption of this structure lies in the bonding interaction between the LUMO (π* orbitals) of these two fragments; moreover, the constraints of the macrocycle probably contribute to the stabilization of this structure.

Introduction

Reduction of aromatic systems by contact with alkali metal is one of the earliest electron-transfer reactions studied in chemistry.[1] It has rapidly been realized that a large variety of ionic species coexist in the reaction medium and that the physical and chemical forms of ion pairs play a decisive role in the chemical behavior of the solution.[2] In this field, the concept of tight or loose ion pairs composed of an aromatic radical anion and a metal cation, eventually separated by solvent molecules, is of central importance.[3] Many studies focused on the constitution of these ion pairs, and it has been shown that several aromatic anions and solvent molecules can be involved in these edifices.[4] In some favorable cases, these species could be crystallized, and for example, the structure of the dimer of

the benzene radical anion potassium-crown ether and of the monomeric toluene radical anion analogue have recently been reported.[5]

A particularly interesting situation occurs when the organic molecule allowed to react with the alkali metal contains two equivalent aromatic subsystems. In this case, communication between these two subsystems increases delocalization of the unpaired electron and can lead to a new type of chemical bond or molecular structure. For example, we have recently shown that reduction of the diphosphacyclophane **1** leads to the formation of an intramolecular one-electron P−P bond.[6]
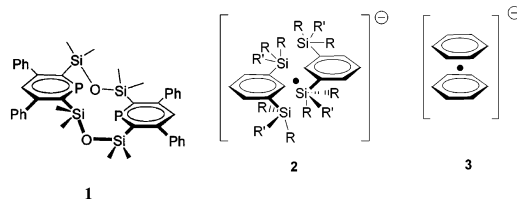
Apparently, this process is made possible by the constraints of the macrocycle which maintain the two CPC moieties in an

---

† University of Geneva.
‡ Ecole Polytechnique.
(1) Lipkin, D.; Paul, D. E.; Townsend, J.; Weissman, S. I. *Science*, **1953**, *117*, 534. Weissman, S. I.; Townsend, J.; Paul, D. E.; Pake, G. E. *J. Chem. Phys*. **1953**, *21*, 2227. De Boer, E. *J. Chem. Phys.* **1956**, *25*, 190.
(2) Szwarc, M. *Acc. Chem. Res.* **1969**, *2*, 87.
(3) Szwarc, M. *Acc. Chem. Res.* **1972**, *5*, 169. Dye, J. L. *Angew. Chem., Int. Ed. Engl.* **1979**, *18*, 587.
(4) Bock, H.; Näther C.; Ruppert, K.; Havlas, Z. *J. Am. Chem. Soc.* **1992**, *114*, 6907. Bock, H.; Ansari, M.; Nagel, N.; Havlas, Z. *J. Organomet. Chem.* **1995**, *499*, 63. Bock, H.; Herrmann H.-J. *J. Am. Chem. Soc.* **1989**, *111*, 7622.

(5) Hitchcock, P. B.; Lappert, M. F.; Protchenko, A. V. *J. Am. Chem. Soc.* **2001**, *123*, 189.
(6) Cataldo, L.; Choua, S.; Berclaz, T.; Geoffroy, M.; Mézailles, N.; Ricard, L.; Mathey, F.; Le Floch, P. *J. Am. Chem. Soc.* **2001**, *123*, 6654.

adequate relative orientation. These results prompted us to look for a molecular framework that could stabilize an unpaired electron between two partially superposed phenyl rings as in **2**. Such a system can be seen as a representation of the transition state of an electron transfer (ET) between two disilylbenzene rings according to an inner-sphere mechanism.[7,8]

Electron transfer between two phenyl rings is a fundamental process in chemistry; it was mainly investigated by studying radical anions derived from paracyclophanes.[9,10] Such studies revealed that an electron-hopping process between two superposed rings takes place in systems like **3**, but as far as we know, direct information about the structural modifications induced by the presence of the extra electron could never be directly obtained. Moreover, all the attempts to form the radical anion of the anti[2.2]metacyclophane failed.[11]

We decided therefore to proceed to the one-electron reduction of the system **4** featuring two phenyl rings linked in meta positions by two $-R_2Si-O-SiR_2-$ bridges, this framework being structurally analogous to that used in our experiments with phosphorus derivatives. Although the macrocycle is certainly much more flexible in **4** than in usual [2.2]cyclophanes, the two aromatic rings are expected to remain rather close to each other in two almost parallel planes.

4   **5**
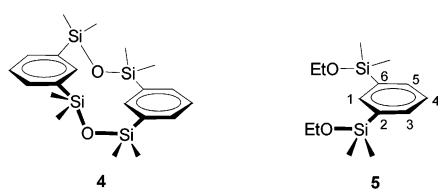
In the present study, we use EPR/ENDOR spectroscopy to identify the one-electron reduction products of **4** and to determine some of the experimental conditions that govern the formation of these species as well as the nature of the ion pairs produced in the reacting medium. The interpretation of the spectra is, in part, based on a comparison between the spin delocalization found for $4^{\bullet-}$ and $5^{\bullet-}$. The structural modifications which accompany the addition of an unpaired electron between the two partially overlapping phenyl rings are rationalized by DFT calculations and, finally, evidenced by the crystal structure of $4^{\bullet-}$. Then, the properties of this structure are examined in order to know to what extent it is consistent with an ET transition state.

Results

1. Reduction of Octamethylcyclo-di(*m*-silylphenylenedisiloxane) 4 and Crystal Structures. The mono electronic reduction of **4** was attempted in two solvents: THF or dimethoxyethane with sodium or potassium metal as reducing agents. In a first series of experiments, these reductions were carried out at room temperature by reacting **4** in solution with an equimolar amount or a slight default of the alkali metal.
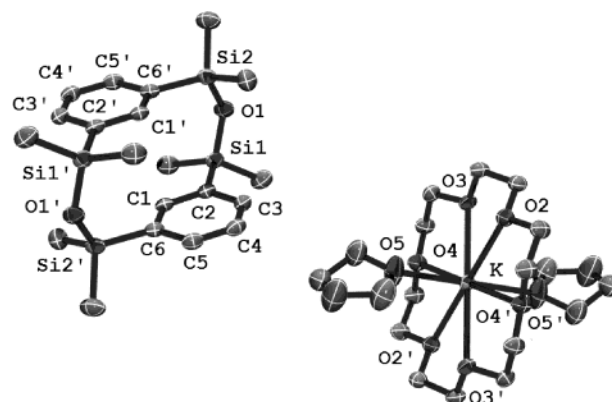
(7) Eberson, L.; Shaik, S. S. *J. Am. Chem. Soc.* **1990**, *112*, 4484.
(8) Kochi, J. K. *Angew. Chem., Int. Ed. Engl.* **1988**, *27*, 1227. Rosokha, S. V.; Kochi, J, K. *J. Am. Chem. Soc.* **2001**, *123*, 8985.
(9) Gerson, F.; Martin, W. B., Jr. *J. Am. Chem. Soc.* **1969**, *91*, 1883.
(10) Gerson, F. *Topics in Current Chemistry*; Vögtle, F., Ed.; Springer: Berlin; p 57.
(11) Attempts to form the radical anion of the anti[2.2]metacyclophane afforded the radical anion of tetrahydropyrene with the concomitant release of H_2. Iwaizumi, M.; Isobe. T. *Bull. Chem. Soc. Jpn.* **1965**, *38*, 1547. Elschenbroich, Ch.; Gerson, F.; Boekelheide, V. *Helv. Chim. Acta* **1971**, *54*, 361.

Figure 1. ORTEP view of the X-ray crystal structure of **6**. This structure is composed of $4^{\bullet-}$ and of [K(18-C-6)(THF)$_2$].

Whereas, no reaction occurred with Na metal, the reaction with K turned dark red after a few minutes and evolved to yield an inhomogeneous dark brown solution. Suspecting that the temperature would probably play an important role on the composition of the reacting medium, we carried out the same experiment at -18 °C. Under these conditions, an homogeneous brown solution slowly formed within 12 h but no crystals could be grown from it. More satisfactory results were obtained by reacting **4** with K metal in a THF/hexane mixture in the presence of 18-crown-6. After 3 days at -18 °C, small dark brown crystals of **6** were formed. Compound **6** turned out to be extremely sensitive toward moisture and oxygen, and crystals could not be analyzed using classical conditions. Protecting them in oil did not prevent their rapid decomposition. They were successfully mounted on the X-ray diffractometer under a stream of argon gas at -18 °C (see the Experimental Section for technical details on the technique used). An ORTEP view of **6** is presented in Figure 1.

As can be seen, the structure of **6** consists of two discrete units: a reduced molecule of **4** and the countercation [K(18-C-6)(THF)$_2$]. To precisely assess the effects of the reduction on the structure of **4**, its structure was recorded under the same conditions (-150 °C) used for **6**. Indeed, the structure of **4** has already been recorded by other authors,[12] but at room temperature. To facilitate this comparison, the metric parameters of both structures are summarized in Table 1. They will be discussed, together with those resulting from structure optimizations in the DFT part (vide infra).

2. Chemical Reduction and EPR Spectra. A pale yellow solution of **4** in THF turned to yellow/orange when in contact with a potassium mirror at 220 K. As shown in Figure 2a, this solution led, at 210 K, to an EPR spectrum characterized by a 20.0 MHz hyperfine interaction with two spin $\frac{1}{2}$ nuclei; each line of the resulting 1−2−1 pattern exhibits smaller additional couplings. The same spectrum was recorded, at 210 K immediately after reaction at 300 K, of a THF solution of **4** on a potassium mirror in the presence or in the absence of crown ether. To identify the numerous hyperfine constants, ENDOR experiments were carried out with this latter solution. The resulting spectrum is shown in Figure 2b; it clearly indicates four different small ^{1}H coupling constants which are reported in Table 2 and which led to a good simulation of the EPR

(12) Zhang, R.; Pinhas, A. R.; Mark, J. E.; Lake, C. H. *J. Inorg. Organomet. Polym.* **1999**, *9*, 63.

Table 1. Calculated and Experimental Geometries[a] for **4** and **4•−**

parameter	neutral molecule **4**		radical anion **4•−**	
	crystal structure	anti conformer (DFT)	from crystal structure of **6**	anti conformer (DFT)
C1···C1′	3.323(3)	3.532	3.089	3.358
C6···C2′	3.676	4.185	3.509	3.830
C5−C6	1.399(2)	1.407	1.435	1.433
C4−C5	1.389(2)	1.395	1.380	1.398
C1−C6	1.402(2)	1.407	1.399	1.408
C2−Si1	1.876(1)	1.891	1.850	1.867
C2−Si1−O1	108.67	110.389	112.1	112.89
Si1−O1−Si2	139.61	151.33	129.22	133.89
ξ[b]	0.0	0.0	0.0	0.0

[a] Distances in Å, angles in degree [b] ξ: angle between the normals to the phenyl rings.
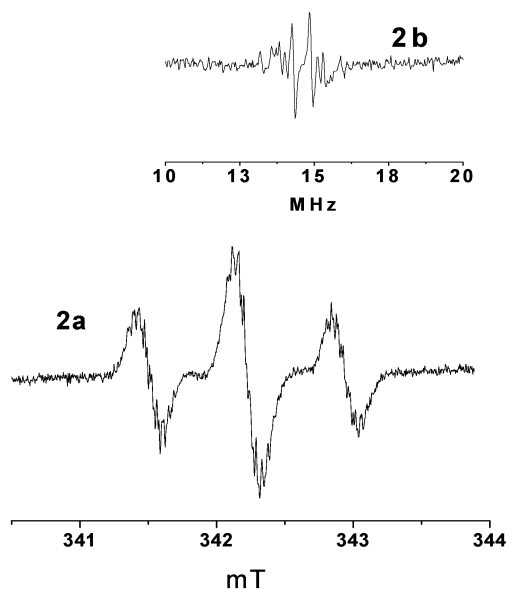

Figure 2. (a) EPR spectrum obtained at 210 K after reaction of a solution of **4** in THF on a potassium mirror. (b) ENDOR spectrum obtained with the same solution.

spectrum.[13] Reduction of **5** is expected to afford the coupling constants of a radical anion delocalized on a single *m*-disilylphenylene moiety. The corresponding EPR spectrum, obtained after reaction of a solution of **5** in THF, at room temperature on a potassium mirror is shown in Figure 3 together with the corresponding ENDOR spectrum obtained at 196 K. The resulting EPR parameters are given in Table 2.

To detect the spectral modifications caused by the presence of crown ether, the following experiments were carried out with THF solutions containing equimolar quantities of **4** and 18-crown-6. The EPR spectrum obtained after reduction with potassium of such a solution, at 200 K, is shown in Figure 4a. Clearly, this spectrum is different from the spectrum shown in Figure 2a. It is characterized by a quintet pattern exhibiting an hyperfine coupling of ≅11 MHz. An additional structure is detected on the five lines, but the resolution of this structure is dependent upon both the position of the transition and the temperature of the sample. Clearly, between 170 and 250 K, transitions 1, 3, and 5 exhibit additional smaller splittings which are not detected with transitions 2 and 4. This temperature dependence was found to be reversible. To ascertain whether a

single species was responsible for the five lines of the quintet, we performed ENDOR measurements by saturating the five lines successively. For each saturating position, the same ENDOR lines were recorded (Figure 4b). The resulting coupling constants are shown in Table 2. They allowed us to reproduce the substructure observed on transition 1, 3 and 5. This variation of the spectrum with temperature is due to the well-known alternating line-width phenomenon. This is caused by a time-dependent mechanism associated with rapid jumps of the electron between two sites exhibiting a same hyperfine structure with two equivalent protons. This is consistent with a hopping of the electron between the two phenyl rings and agrees with the previous observation on paracyclophanes.[10] It can nevertheless be remarked that the fluxionality of the macrocycle could also give rise to an alternating line-width phenomenon by making the proton couplings of the two rings slightly different; interconversion between various conformations of similar macrocycles has recently been detected by NMR.[14] Therefore, we cannot totally exclude this second interpretation.

3. DFT Calculations. A. Systems Containing One Benzene Ring. DFT calculations were performed on **5** and **5•−** in order to assess the structural modifications induced by the reduction of the 1,3-bis(ethoxydimethylsilyl)benzene system. After preliminary MM+ calculations, the geometries of **5** and of its radical anion were optimized by DFT by assuming a *Cs* symmetry. The results show that, besides an increase of ~2.5° in the C3−C4−C5 and C2−C1−C6 bond angles, the one-electron reduction of **5** causes an increase of the C2−C3 (0.06 Å) and C5−C6 bond lengths together with a decrease in the C2−Si (0.054 Å) and C6−Si bond lengths.

These geometrical properties are consistent with the MO shown in Figure 5: in the neutral compound, four carbon atoms participate in the HOMO (called π_1) which is bonding between C2 and C3 and between C5 and C6, while the HOMO-1 (called π_2) is delocalized on the six carbons and is bonding among C2−C1−C6 and among C3−C4−C5. In the radical anion, the SOMO corresponds to the antibonding orbital π_1* consistent with the increase in the C2−C3 and C5−C6 bond lengths. This SOMO is bonding between carbon and silicon, in accord with the shortening of the C2−Si and C6−Si bonds. The various proton isotropic coupling constants are reported in Table 3. In accord with the SOMO shown in Figure 5, the salient feature is a large hyperfine interaction (30 MHz) with the two protons bound to C3 and C5.

B. Systems Containing Two Benzene Rings. Two main types of structures can be envisaged for **4**: the syn and the anti

(13) Probably due to a too low intensity, the high-frequency signal (corresponding to an hyperfine coupling of ~20 MHz) is not observed on the ENDOR spectrum. Nevertheless, the corresponding splitting is clearly measured on the EPR spectrum.

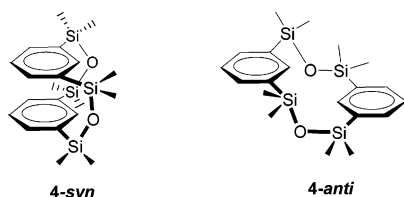(14) Mitchell, R. H. *J. Am. Chem. Soc.* **2002**, *124*, 2352.

Table 2. Experimental Isotropic [1]H Coupling Constants for the Reduction Products of **4** and **5**

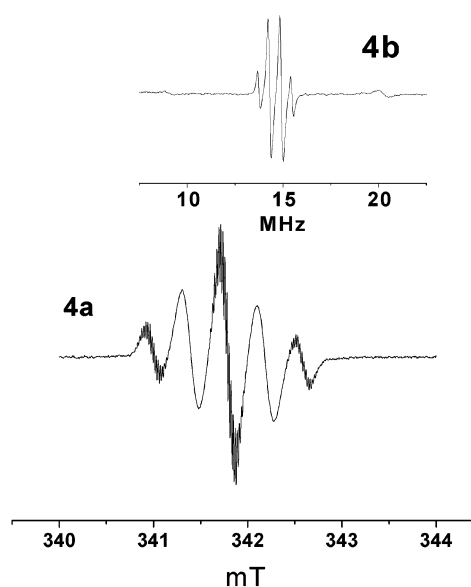| compd | experimental conditions | coupling constants[a] with proton in position (MHz) | | | | |
		3,5	4	Me(Si)	1	Me(Si′)
4	without crown ether, reaction at 220 K or 300 K	20.8(×2)	1.93(×1)	1.46(×12)	1.04(×1)	0.57(×12)
	with crown ether, reaction at 300 K	20.02(×2)	2.00(×1)	1.46(×12)	1.07(×1)	0.57(×12)
4	with crown ether, reaction at 200 K	11.42(×4)	1.77(×2)	0.61(×24)		
5	without crown ether, reaction at rt	21.00(×2)	2.80(×1)	1.08(×12)	0.65(×1)	0.23(×4)

[a] The coupling constants are measured from ENDOR spectra, and the number of equivalent protons is obtained after simulation of the EPR spectra; the number of equivalent protons is given in parentheses. The positions of the protons are determined after comparison with DFT results.
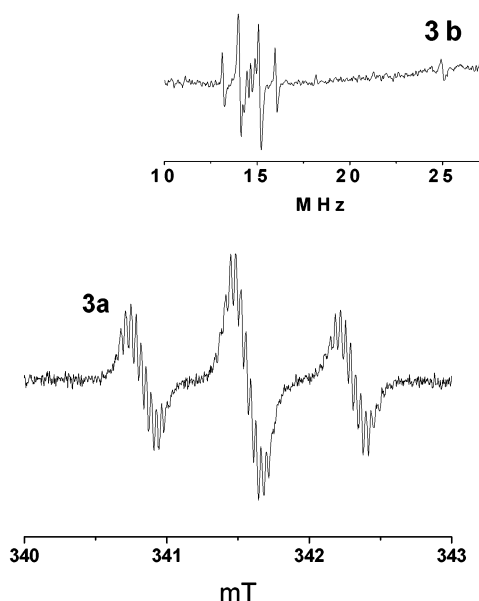
Figure 3. (a) EPR spectrum obtained at room temperature after reaction of a solution of **5** in THF on a potassium mirror. (b) ENDOR spectrum obtained with the same solution.

Figure 4. (a) EPR spectrum obtained at 200 K after reaction on a potassium mirror, at 200 K, of a solution containing equimolar quantities of **4** and 18-crown. (b) ENDOR spectrum obtained with the same solution.

conformers (**4-syn** and **4-anti**). Although the molecule can possibly wobble between a great number of conformers,[14] we have limited our calculations to the minimum energy syn and anti conformers found after a geometry optimization which assumes $C2$ symmetry. Since the crystal structures of both the neutral and the anionic species correspond to the anti conformers, the calculated geometrical parameters are reported in Table 1 for these conformers only (the parameters calculated for the syn isomers are given as Supporting Information). For both the neutral molecule and the radical anion, the energy of the anti conformer is found to be lower than that of the syn conformer: $(E_{syn} - E_{anti})$ is equal to 1.449 kcal mol^{-1} for **4** and to 7.175 kcal mol^{-1} for **4**[·−].

As shown in Table 1, the geometries calculated for the neutral and anionic anti conformers agree with those measured from the crystal structures. Nevertheless, some differences exist in

the Si−O−Si bond angles which are smaller in the experimental structures than in the optimized geometries. This leads to interphenylene distances which are shorter for the crystallographic structures than for the DFT optimized geometries: for example, the difference $\Delta_{C1C1'}$ ($\Delta_{C1C1'} = C1C1'_{DFT} - C1C1'_{crystal}$) is equal to 0.209 Å and 0.269 Å for **4** and **4**[·−], respectively, while the corresponding values $\Delta_{C2C2'}$ are equal to 0.509 Å and 0.321 Å, respectively. These differences are possibly due to packing effects in the crystal. The important point shown by Table 1 concerns the structure modifications induced by the one-electron reduction of **4**. DFT geometries, as well as crystal structures, show that by passing from the neutral molecule to the radical anion two main modifications appear: (1) a deformation of the phenylene rings which remain planar but undergo an increase in the C2−C3,C5−C6 (and C2′−C3′,C5′−C6′) distances ($\Delta_{anion-neutral}$ is equal to 0.026 Å for the DFT geometries and 0.034 Å for the crystals) and (2) a drastic shortening of the distance between the two phenylene rings. The DFT calculated C1··C1′ distance decreases by 0.174 Å (0.234 Å for the crystal), while the C6−C2′ and C2−C6′ DFT distances decrease by 0.355 Å (0.167 Å for the crystal); consistent with this diminution in the interphenylene distance, a spectacular decrease in the Si−O−Si angles (17.44° by DFT, 10.39° in the crystal) occurs by passing from the neutral to the anionic species. Also noteworthy is the shortening of the C−Si
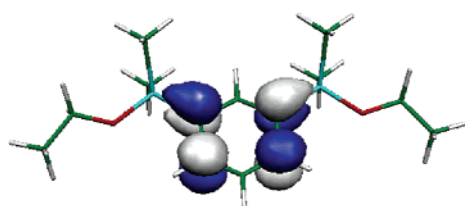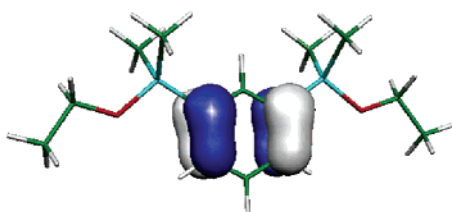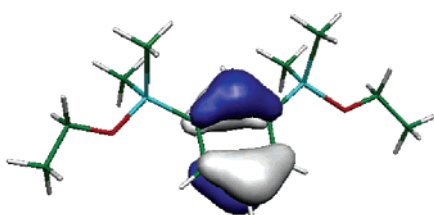
NEUTRAL → RADICAL ANION

LUMO (π_1^*) → SOMO

HOMO (π_1) → SOMO-1

HOMO-1 (π_2) → SOMO-2

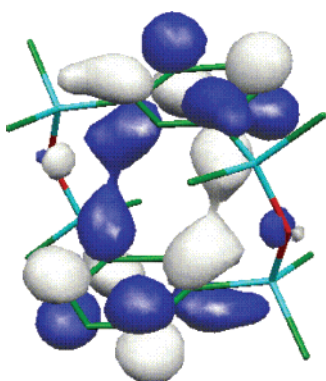**Figure 5.** Representation of the molecular orbitals for **5** and its radical monoanion (cutoff = 0.0500).

Figure 6. Representation of the SOMO for **4**•⁻ (cutoff = 0.0349).

bond. Similar effects are calculated for the syn conformer and are given as Supporting Information.

DFT calculations clearly indicate that the positive atomic spin densities are mainly found on carbon atoms C3, C5, C3′, and C5′ and in a smaller extent on the four silicon atoms and the carbons atoms C2,C6, C2′, and C6′. A representation of the SOMO is shown in Figure 6, while three other occupied MOs

Table 3. Calculated ¹H Isotropic Coupling Constants[a] (MHz)

radical anion	H3,5 (3′,5′)	H4 (4′)	H1 (1′)	Si–CH₃[b]	Si–CH₃	CH₂–Me
5•⁻	−30.3	6.88	0.99	1.57	1.57	0.19
4•⁻	−13.81	3.11	0.405	0.83	0.88	

[a] Values in parentheses correspond to the additional protons for **4**•⁻. [b] Averaged value for the three protons of each methyl group; two sets of four equivalent methyl groups in **4**•⁻ and two sets of two equivalent methyl groups in **5**•⁻.

are presented in Figure 7 for both **4** and its radical monoanion. The calculated isotropic ¹H coupling constants are given in Table 3.

Discussion

As shown in Figure 5, the SOMO of the radical anion of **5**•⁻ is mainly constructed from the $2p_z$ orbitals of the C2,C3, C5, and C6 carbon atoms and, to a smaller extent, from the silicon p_z orbitals. Consistent with the composition of this SOMO, the EPR spectrum of **5**•⁻ shown in Figure 3 exhibits a large coupling with the two protons bound to carbons in positions 3 and 5. Although the coupling constants calculated by DFT are rather larger than the experimental ones, the accord can be considered as reasonable. The fact that the reaction of **4** on a potassium mirror in the absence of crown ether leads to EPR/ENDOR spectra which are very similar to those obtained by reduction of **5** (Table 2) indicates that, in these conditions, the radical anion remains localized on only one of the two benzene moieties of **4**. In both cases, a tight ion pair K⁺····[RC₆H₄R]•⁻, stabilized by the electrostatic attractive interaction E_a, is probably formed. In the presence of crown ether, however, the principal coupling constants are divided by 2 and the number of each class of protons participating in the hyperfine structure is multiplied by two. These new coupling constants are quite similar to those calculated by DFT for **4**•⁻ (Table 3). They clearly indicate that, in the presence of crown ether, the odd electron is equally delocalized on both phenyl rings of **4**•⁻. An interpretation of this result is sketched in Scheme 1. When K⁺ is embedded inside the crown ether, the tight ion pair K⁺····[RC₆H₄R]•⁻ is replaced by a loose pair; E_a almost vanishes, allowing the structure of the radical anion to relax to a conformation stabilized by intramolecular interactions between the two arene moieties (Scheme 1).

The nature of this interaction is clearly seen from the MO represented in Figures 7 and 8. In the neutral molecule **4**, the HOMO results from the antibonding interaction between the π_2 MO of each "monomer" (Figures 7a, 8a), while the HOMO-1 and HOMO-2 correspond to the antibonding and bonding interaction between the π_1 MO, respectively. The overlaps between orbitals localized on carbons C1,C2, C6 and C1′,C2′, C6′ lead in the neutral molecule to a short C1···C1′ distance (3.32 Å in the crystal). These four occupied MOs (HOMO, HOMO-1, HOMO-2, HOMO-3) are all close in energy, whereas the LUMO is considerably higher. As shown in Figures 6 and 8b, in the radical anion **4**•⁻, the SOMO results from a bonding interaction between the π_1^* orbitals. Consistent with this SOMO composition, the crystal structure of **6** indicates that the one-electron reduction of **4** is accompanied by a shortening of the interphenyl distances and a lengthening of the C2−C3, C5−C6 bond lengths. It can also be remarked that addition of the extra electron has inversed the order of the HOMO and HOMO-1 mentioned for the neutral molecule.
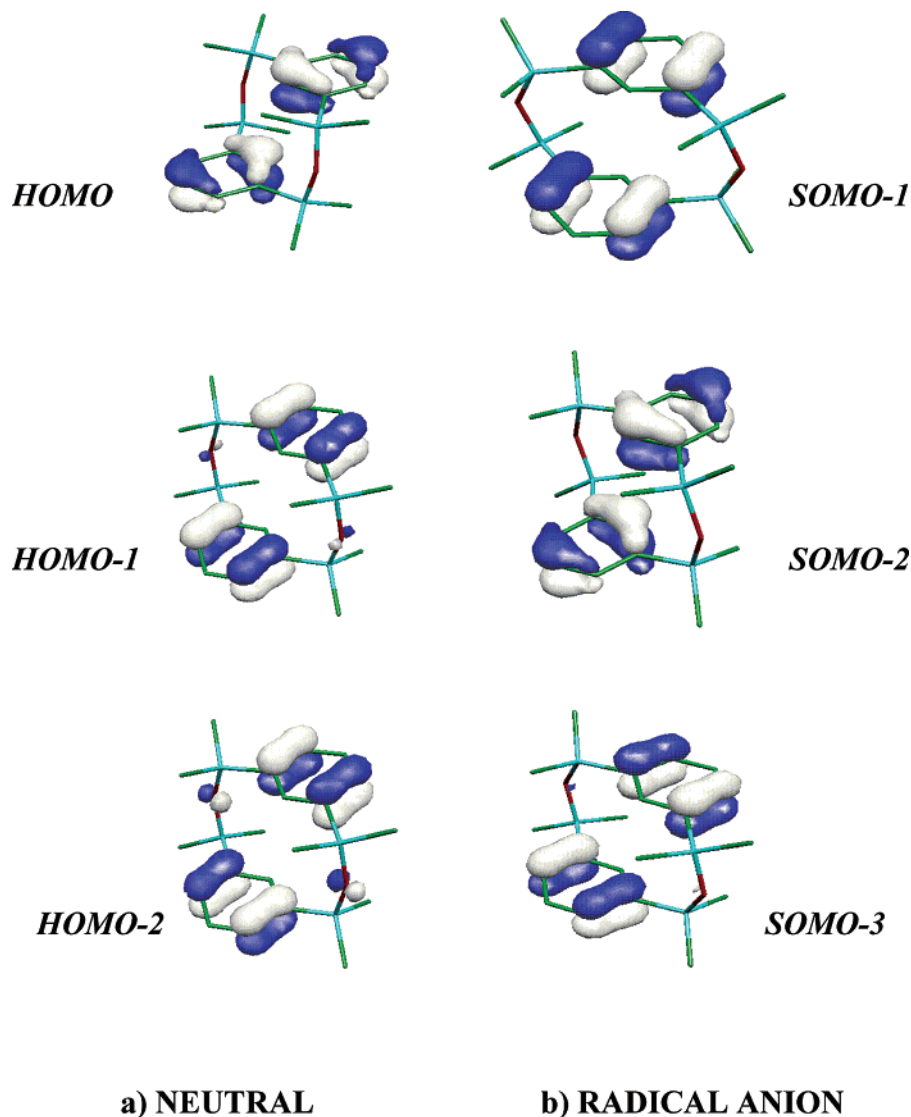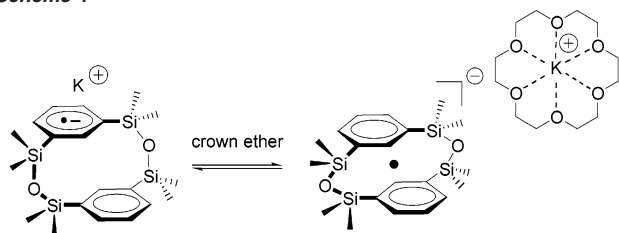
HOMO

SOMO-1

HOMO-1

SOMO-2

HOMO-2

SOMO-3

a) **NEUTRAL**   b) **RADICAL ANION**

Figure 7. Representation of the molecular orbitals for **4** and **4$^{\bullet-}$** (cutoff = 0.0500).

Scheme 1

Interaction between π^* orbitals of monomers has been invoked to explain the dimerization of the diphosphirenyl radical[15] and the formation of other dimeric structures such as in Cl$_4$$^{+}$[16] and Cl$_2O_2$$^{+}$.[17] In K$_2$[TCNE]$_2$, recently described by Novoa et al., [18] the attractive electrostatic interactions "cation$\cdots$[TCNE]$^-$" enable the overlap of the SOMOs of the [TCNE]$^-$ monomers through four carbon atoms and lead to intradimer C$-$C distances ($\geq$2.8 Å) which are substantially less
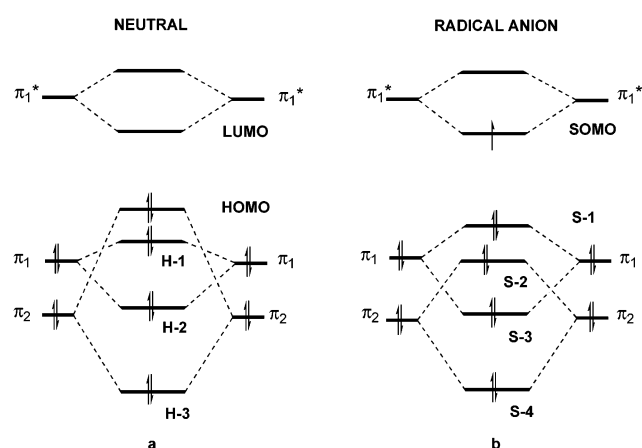
(15) Canac, Y.; Bourissou, D.; Baceiredo, A.; Gornitzka, H.; Schoeller, W. W.; Bertrand, G. *Science* **1998**, *279*, 2080.
(16) Seidel, S.; Seppelt, K. *Angew. Chem., Int. Ed.* **2000**, *39*, 3923.
(17) Drews, T.; Koch, W.; Seppelt, K. *J. Am. Chem. Soc.* **1999**, *121*, 4379.
(18) Novoa, J. J.; Lafuente, P.; Del Sesto, R. E.; Miller, J. S. *Angew. Chem., Int. Ed.* **2001**, *40*, 2540.

NEUTRAL   RADICAL ANION

Figure 8. Formation of the molecular orbitals of **4** (and **4$^{\bullet-}$**) from the π-type orbitals of **5**.

than the π-C van der Waals radius (3.40 Å). These features are rather different from those observed in our case: the crystal structure of **6** shows that the countercation is far from the **4$^{\bullet-}$** unit and does not seem to contribute to its stabilization. Moreover, the interphenylene carbon$-$carbon distances are rather longer than the intradimeric C$\cdots$C distances observed in
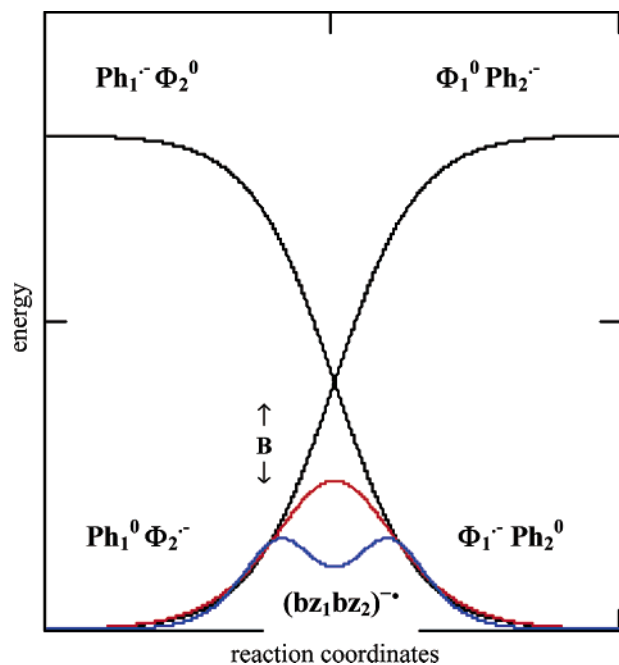
Figure 9. Diagram for the electron transfer between the two phenyl rings of **4**. The red curve illustrates the transition state between the two phenylene rings in the absence of the bridge between the two silicon atoms. The minimum observed on the blue curve is attributed to constraints in the macrocycle.

$K_2[TCNE]_2$ (the shortest distance is equal to 3.089 Å). In fact, the structure of **4**[•−], in the presence of crown ether, is a model for the transition state of an inner-sphere ET between two partially overlapping *m*-phenylene rings marked 1 and 2:

$$Ph_1{}^0\Phi_2{}^{•-} \rightarrow \Phi_1{}^{•-}Ph_2{}^0$$
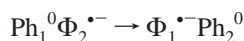
where Ph and Φ correspond to the relaxed geometries of the neutral and anionic phenylene group, respectively.[19] In a first approximation, the role of the Si−O−Si moieties in this process is mainly to avoid a separation between the two phenylene rings after the electron transfer has occurred and, thus, to lead to the electron hopping phenomenon. Referring to Figure 9 and in accord with the study of Eberson and Shaik,[7] we find the transition state, located at the top of the red curve, is characterized by the resonance $(bz_1{}^0bz_2{}^-) \leftrightarrow (bz_1{}^- bz_2{}^0)$, where bz represents the geometry of the phenylene ring in the transition state. The corresponding resonance interaction B is directly related to the overlap of the two $\pi_1{}^*$ orbitals described previously. The interphenylene carbon−carbon distances measured on the crystal structure of **4**[•−] (Table 1) are in excellent agreement with this interpretation, since the values expected for the transition state of an inner-sphere electron transfer are comprised between 3.0 and 3.5 Å.

It is nevertheless possible that the silicon-containing spacers play an additional role in this mechanism. Indeed, the vibration analysis of the DFT optimized geometry indicates that the corresponding structure is a real minimum, suggesting that the $(bz_1bz_2)^{-•}$ structure is a metastable state, as shown by the blue curve of Figure 9. The presence of this local minimum is likely to be due to additional interactions caused by the macrocycle.

(19) The geometrical changes caused by addition of an electron to the *m*-disilylbenzene can be evaluated from the DFT optimized structures of **5** and **5**[•−] given in the Supporting Information.

With regard to the influence of the silicon atoms, it is worthwhile mentioning that the presence of these heteroatoms probably affects the composition and the overlap of the various π and π* orbitals and therefore contribute to the electron-transfer process (cf. value of B in Figure 9).

Concluding Remarks

EPR/ENDOR measurements have shown that, in conditions preventing the formation of tight ion pairs, the reduction of **4** leads to the formation of a radical anion whose unpaired electron is equally delocalized on the two *m*-phenylene rings of this molecule and which undergoes a dynamical process. The crystal structure of this radical anion clearly indicates that the reduction of **4** decreases the distance between the two phenylene rings, leading to a structure which is a model for the transition state of an electron transfer between two *m*-phenylene moieties. As shown by DFT, and in accord with the experimental hyperfine couplings, this structure results from an overlap between the LUMO of the two $(R'R_2Si)_2Ph$ moieties in **4**, with an almost negligible contribution of the Si−O−Si links to the MO involved in the electron-transfer process. It can therefore be foreseen that, in a solution containing isolated $(R_3Si)_2Ph$ molecules and $[(R_3Si)_2Ph]^{•-}$ radical anions, the electron transfer between these two systems would be characterized by a transition state very close to **4**[•−]. This agrees with previous studies[7] which proposed that organic ET reactions of radical ions proceed through relatively compact transition states and, generally, follow an inner-sphere mechanism.

Experimental Section

Apart from the synthesis of **4** that can be carried out under classical conditions, all reductions were performed in the glovebox. THF and hexane were distilled twice on Na/benzophenone and stored in the glovebox on molecular sieves (4 Å). Compound **4** was prepared according to a published procedure.[20]

Reduction of 4. In the glovebox, a tube was successively charged with **4** (50 mg, 0.12 mmol), the 18-crown-6 (32 mg, 0.12 mmol), and a mixture of THF/hexane (0.5 mL/0.5 mL). A thin piece of potassium metal (3 mg, 0.077 mmol) was added, and the tube was rapidly sealed under vacuum and then stored in the freezer at −18 °C. After 3 days, the tube was rapidly warmed to room temperature and introduced in the glovebox. After a rapid filtration and drying, the collected crystals were weighed as fast as possible because **6** decomposes at room temperature. Yield: 43 mg (50%).

The same experiment was carried out in DME, but no crystal could be obtained from this solvent.

X-ray Crystallographic Studies of 4 and 6. Crystals of **4** (triclinic, space group $P\bar{1}$) were obtained in ether at −18 °C. Crystals of **6** (triclinic, space group $P\bar{1}$) were obtained as described previously from a cooled solution of the radical anion in a mixture of THF/hexane (1:1). After the tube was warmed to room temperature, it was broken, and the mother liquor and crystals were poured onto an absorbing paper under a stream of argon at −20 °C. The device used for collecting crystals consists of a long glass tube, bevelled at one extremity; this tube is connected to a Dewar of liquid nitrogen, and a pressured stream of argon allows the diffusion of cold argon in the tube. By this way, crystals which are deposited at the end of the tube can be observed for some time without apparent decomposition. Data were collected on an Enraf−Nonius Kappa CCD diffractometer using an Mo Kα X-ray source and a graphite monochromator. Experimental details are given as Supporting Information. The crystal structures were solved using

(20) Zhang, R.; Pinhas, A. R.; Mark, J. E. *Polym. Prepr.* (*Am. Chem. Soc., Div. Polym. Chem.*) **1998**, *39*, 607.

SIR 97,[21] and Shelxl-97.[22] ORTEP drawings were made using ORTEP III for Windows.[23]

EPR/ENDOR Experiments. EPR and ENDOR experiments were carried out on a 200D Bruker and a 300 Bruker spectrometer, respectively (X-band, 100 kHz field modulation). Potassium mirrors were formed by sublimation of the metal under high vacuum, and the sample tubes were sealed before contact of the reacting solution (generally 10^{-2} M) on the mirror.

DFT Calculations. DFT calculations were performed by using the Gaussian 98 package.[24] We employed the B3LYP functional[25,26] and triple-ζ basis sets (6-31G* and 6-31+G* for the neutral molecules and the radical anion, respectively). The optimized structures were char-

acterized by harmonic frequency analysis as minima (all frequencies real).[27] The molecular orbitals were represented by using the Molekel program.[28]

Supporting Information Available: Comparison of metric parameters between the crystal structures of **4** and **6**, optimized geometries for **5** and **5**$^{\bullet-}$ (DFT calculations), optimized parameters for **4-*syn*** and **4-*syn*$^{\bullet-}$** (DFT calculations), and simulations of the EPR spectra by using the ENDOR frequencies. Table of crystal data, table of atomic coordinates and equivalent isotropic displacement parameters, table of bond lengths and bond angles, table of anisotropic displacement parameters, and the table of hydrogen coordinates and isotropic displacement parameters for the structure of **6** are also given as well as a table of crystal data for **4**. This material is available free of charge via the Internet at http://pubs.acs.org.

JA0209060

(21) Altomare, A.; Burla, M. C.; Camalli, M.; Cascarano, G.; Giacovazzo, C.; Guagliardi, A.; Moliterni, A. G. G.; Polidori, G.; Spagna, R. *SIR 97*, an integrated package of computer programs for the solution and refinement of crystal structures using single-crystal data; 1999. (See: *J. Appl. Crystallogr.* **1994**, *27*, 435.)

(22) Sheldrick, G. M. *SHELXL-97*; Universität Göttingen: Göttingen, Germany, 1998.

(23) Farrugia, L. J. *ORTEP III* (Department of Chemistry, University of Glasgow); *J. Appl. Cryst.* **1997**, *30*, 565−567.

(24) Frisch, M. J.; Trucks, G. W.; Schlegel, H. B.; Scuseria, G. E.; Robb, M. A.; Cheeseman, J. R.; Zakrzewski, V. G.; Montgomery, J. A.; Stratmann, R. E.; Burant, J. C.; Dapprich, S.; Millam, J. M.; Daniels, A. D.; Kudin, K. N.; Strain, M. C.; Farkas, O.; Tomasi, J.; Barone, V.; Cossi, M.; Cammi, R.; Mennucci, B.; Pomelli, C.; Adamo, C.; Clifford, S.; Ochterski, J.; Petersson, G. A.; Ayala, P. Y.; Cui, Q.; Morokuma, K.; Malick, D. K.; Rabuck, A. D.; Raghavachari, K.; Foresman, J. B.; Cioslowski, J.; Ortiz, J. V.; Stefanov, B. B.; Liu, G.; Liashenko, A.; Piskorz, P.; Komaromi, I.; Gomperts, R.; Martin, R. L.; Fox, D. J.; Keith, T.; Al-Laham, M. A.; Peng, C. Y.; Nanayakkara, A.; Gonzalez, C.; Challacombe, M.; Gill, P. M. W.; Johnson, B. G.; Chen, W.; Wong, M. W.; Andres, J. L.; Head-Gordon, M.; Replogle, E. S.; Pople, J. A. *Gaussian 98*, revision A.7; Gaussian, Inc.: Pittsburgh, PA, 1998.

(25) Becke, A. D. *J. Chem. Phys.* **1993**, *98*, 5648.

(26) Lee, C.; Yang, W.; Parr. R. G. *Phys. Rev. B* **1988**, *54*, 785.

(27) Except for the ethoxy moiety, the geometry optimized for **5**$^{\bullet-}$ was the same as the geometry optimized for the radical anion of (Me$-$O$-$Si(Me$_2$))$_2$C$_6$H$_4$ which contains a methyl group instead of an ethyl group. The frequency analysis was performed on the methoxy-containing anion.

(28) Flukiger, P. Development of Molecular Graphics Package MOLEKEL, Ph.D. Thesis, University of Geneva, Switzerland, 1992.